24th COBEM - 2017

24th ABCM International Congress of Mechanical Engineering
December 3-8, 2017, Curitiba, PR, Brazil

COBEM-2017-2477
MODAL TESTING OF A FLEXIBLE WING UAV

David Fernando Castillo Zúñiga
Luiz Carlos Sandoval Góes
Raphaela Barbosa
Technological Institute of Aeronautics (ITA), Comando-Geral de Tecnologia Aeroespacial (CTA), 12228-904 - São Jose dos Campos-SP-Brazil
davidfer@ita.br
goes@ita.br
machado@ita.br

Benedito Maciel
Igor Drago
Flight Technologies LTDA, São José dos Campos-SP-Brazil
bcomaciel@flighttech.com.br
igor.drago@flighttech.com.br

Abstract. *This paper presents a methodology to determine the experimental modal characteristics of a flexible wing Unmanned Autonomous Vehicle (UAV). The aircraft is a composite material made UAV, with a 4 meters wing span, high aspect ratio and high structural flexibility. Usually the modal characteristics of an aircraft are obtained experimentally by means of a Ground Vibration Test (GVT), which in turn could be used to correlate and update numerical FEM models to characterize the aeroelastic properties of the aircraft. Typically, this kind of test is carried out using accelerometers as the main type of transducer, but use of strain measurement methods has been increasing in popularity. By using strain measurements, one can not only obtain the modal properties of the structure, but also determine where there are higher levels of stress. This paper describes an ongoing research using accelerometer-based GVT for the wing of the flexible UAV and presents the setup and methodology for a combined accelerometer-strain sensor modal testing configuration.*

Keywords: *Modal Analysis, UAV, Strain Modal Analysis, Experimental Modal Analysis, GVT.*

1. INTRODUCTION

Modal testing is a very important stage in aircraft development and certification analysis, especially to determine the aircraft structural dynamics as an initial step in the aeroelastic analysis. The modal properties of interest are the natural frequencies, the modal shapes, damping and modal mass of the flexible wing structure. Traditionally, the modal properties are estimated by standard Experimental Modal Analysis (EMA) that uses accelerometers and other displacement sensors. This classical approach is described by Ewins (2000) and Maia and Silva (1997). In more recent years there has been a growing interest in Strain Modal Analysis (SMA) (Manzanato *et al*, 2014 and dos Santos, 2015). This methodology is justified by some benefits and advantages of SMA, such as the possibility to obtain directly the modal strain field without the need of further transformations, the applicability to structural health monitoring, and the ability to identify modal parameters in locations where a motion sensor would not be suitable. Nonetheless, this method has some limitations such as the direct determination of a mass normalization using only the strain sensors.

Castillo-Zúñiga and Góes (2012, 2013) applied a traditional GVT to the Vector-P, a medium size UAV built with composite material, to determine its modal properties and aeroelastic characteristics. More recently Santos *et al* (2015) presented the results of a GVT campaign on an F-16 aircraft, where the full aircraft was instrumented with accelerometers and one of the wings was fully instrumented with dynamic strain sensors. They processed simultaneously both strain sensor and accelerometer measurements obtaining strain and displacement mode shapes.

The focus of this paper is to characterize the modal response of the flexible wing UAV. It is a UAV built with composite material, with a 4 meters wing span, high aspect ratio and high structural flexibility. The flexible UAV is illustrated in Fig. 1.

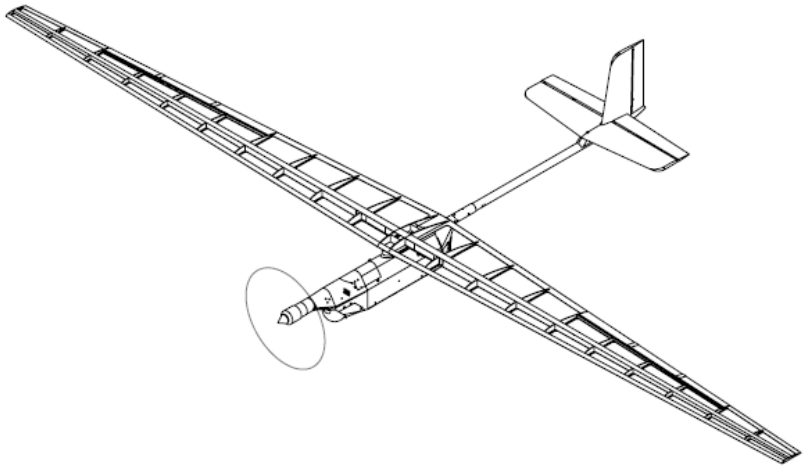

Figure 1. Flexible UAV.

2. THEORETICAL BACKGROUND

2.1 Experimental Modal Analysis (EMA)

The theory of Experimental Modal Analysis (EMA) is well known and can be found in Ewins (2000) and Maia and Silva (1997). In classical modal analysis, the modal properties are obtained from the measurement of Frequency Response Functions (FRF) that defines the relationship between input and output data. The frequency response function relating displacement and force can be expressed in terms of it pole-residue relation as shown in Eq. (1):

$$\boldsymbol{H}(j\omega)=\sum_{r=1}^{n}\frac{Q_r\phi_r\phi_r^T}{j\omega-\lambda_{\omega r}}+\frac{Q_r^*\phi_r^*\phi_r^{*T}}{j\omega-\lambda_{\omega r}^*} \tag{1}$$

where n is the number of considered modes, r is the rth mode, j is the imaginary unit, ω is the frequency variable, $\lambda_{\omega r}$ is the pole of the rth mode, Q_r is the scaling factor, ϕ_r is the rth modal vector, the superscript * is the complex conjugate and the superscript ^{T} is the transpose.

For undamped systems, the frequency response function has a simplified form:

$$\boldsymbol{H}(j\omega)=\sum_{r=1}^{n}\frac{j2\omega_r Q_r\phi_r\phi_r^T}{\omega_r^2-\omega^2} \tag{2}$$

It can be expanded as:

$$\begin{bmatrix} H_{11} & H_{12} & \cdots & H_{1N_q} \\ H_{21} & H_{22} & \cdots & H_{2N_q} \\ \vdots & \vdots & \vdots & \vdots \\ H_{N_p1} & H_{N_p2} & \cdots & H_{N_pN_q} \end{bmatrix} = \sum_{r=1}^{n}\frac{j2\omega_r Q_r}{\omega_r^2-\omega^2}\cdot\begin{bmatrix} \phi_{1r}\phi_{1r} & \phi_{1r}\phi_{2r} & \cdots & \phi_{1r}\phi_{N_qr} \\ \phi_{2r}\phi_{1r} & \phi_{2r}\phi_{2r} & \cdots & \phi_{2r}\phi_{N_qr} \\ \vdots & \vdots & \vdots & \vdots \\ \phi_{N_pr}\phi_{1r} & \phi_{N_pr}\phi_{2r} & \cdots & \phi_{N_pr}\phi_{N_qr} \end{bmatrix}_{N_p\times Nq} \tag{3}$$

where N_p represents the number of output measurements and Nq represents the number of inputs.

The measured FRFs are used for the extraction of the modal parameters with an identification method. In this study it is used the POLIMAX method (Peeters *et al*, 2004).

2.2 Strain Modal Analysis (SMA)

In Strain Modal Analysis (SMA), one defines the strain modes ψ_r that are obtained by application of a differential spatial operator S in displacement mode vectors ϕ_r as shown (dos Santos, 2015):

$$\psi_r = S \cdot \phi_r \tag{4}$$

We obtain an analog expression for the Strain Frequency Response Function (SFRF) for the undamped model:

$$\boldsymbol{H}^{\varepsilon}(j\omega) = \sum_{r=1}^{n} \frac{j2\omega_r Q_r \psi_r \phi_r^T}{\omega_r^2 - \omega^2} \tag{5}$$

which can be expanded as:

$$\begin{bmatrix} H^{\varepsilon}_{11} & H^{\varepsilon}_{12} & \cdots & H^{\varepsilon}_{1N_q} \\ H^{\varepsilon}_{21} & H^{\varepsilon}_{22} & \cdots & H^{\varepsilon}_{2N_q} \\ \vdots & \vdots & \vdots & \vdots \\ H^{\varepsilon}_{N_p1} & H^{\varepsilon}_{N_p2} & \cdots & H^{\varepsilon}_{N_pN_q} \end{bmatrix} = \sum_{r=1}^{n} \frac{j2\omega_r Q_r}{\omega_r^2 - \omega^2} \cdot \begin{bmatrix} \psi_{1r}\phi_{1r} & \psi_{1r}\phi_{2r} & \cdots & \psi_{1r}\phi_{N_qr} \\ \psi_{2r}\phi_{1r} & \psi_{2r}\phi_{2r} & \cdots & \psi_{2r}\phi_{N_qr} \\ \vdots & \vdots & \vdots & \vdots \\ \psi_{N_pr}\phi_{1r} & \psi_{N_pr}\phi_{2r} & \cdots & \psi_{N_pr}\phi_{N_qr} \end{bmatrix}_{N_p \times Nq} \tag{6}$$

There are some particularities for the SFRF matrix. It is not symmetrical and therefore it is not possible to guarantee the reciprocity properties. It is inferred from Eq. (6) that any column of the SFRF matrix contain all information about strain modes (ψ) and any row of the SFRF matrix contain all information about displacement modes (ϕ).

Because the similarity between FRF and SFRF formulation, the same identification methods can be used for both accelerometers and strain modal approaches (dos Santos, 2015).

3. WING TRADITIONAL GVT SETTINGS

Some traditional modal test campaigns were run for the wing of the flexible UAV aiming to define a preliminary position for the acceleration and strain sensors for the complete flexible wing structure. In order to identify the first modes of bending and twisting of the structure, 13 accelerometers ICP model 353B34 were distributed as shown in Fig.2, in a free-free configuration.

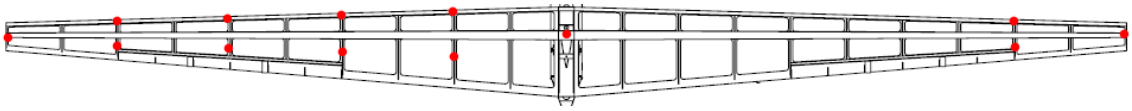

Figure 2. Placement of accelerometers on the free-free configuration.

The excitation of the wing structure is done with an electromagnetic shaker. The interconnection was made by means of a compliant rod or stinger. A power transducer, PCB model 208C02 type ICP is incorporated in the stem. The system used for data acquisition and signal conditioning was the SCADAS III LMS. The hardware and overall layout of the GVT in the free configuration are shown in Fig. 3. The mass of the wing assembly and base is approximately 1844 g.

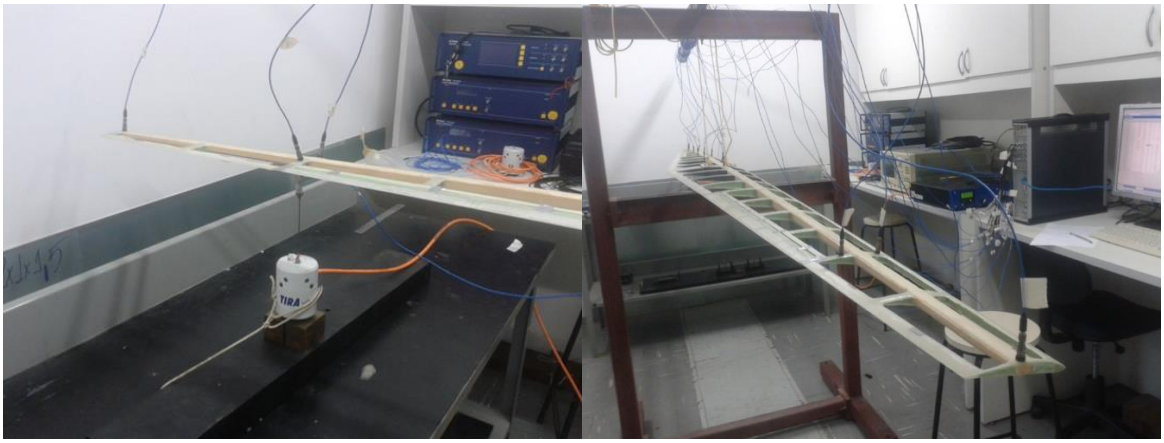

Figure 3. General configuration of the flexible wing in a free-free GVT setup.

For the calculation of FRFs, the spectral parameters are shown in Table. 1. Figure 4 shows the FRF for the driving point in the range of 3 to 60 Hz. Due to the high number of averages, the calculated FRFs are quite smooth. For identification, the POLIMAX method of the LMS software was used, which is a complex least squares method in the frequency domain.

Table 1. FRF Spectral Parameters.

Excitation	Estimator	Averages	Windowing	Bandwidth	Spectral lines	Resolution
Burts Random	H1	50	Hanning	80 Hz	522	0.153 Hz

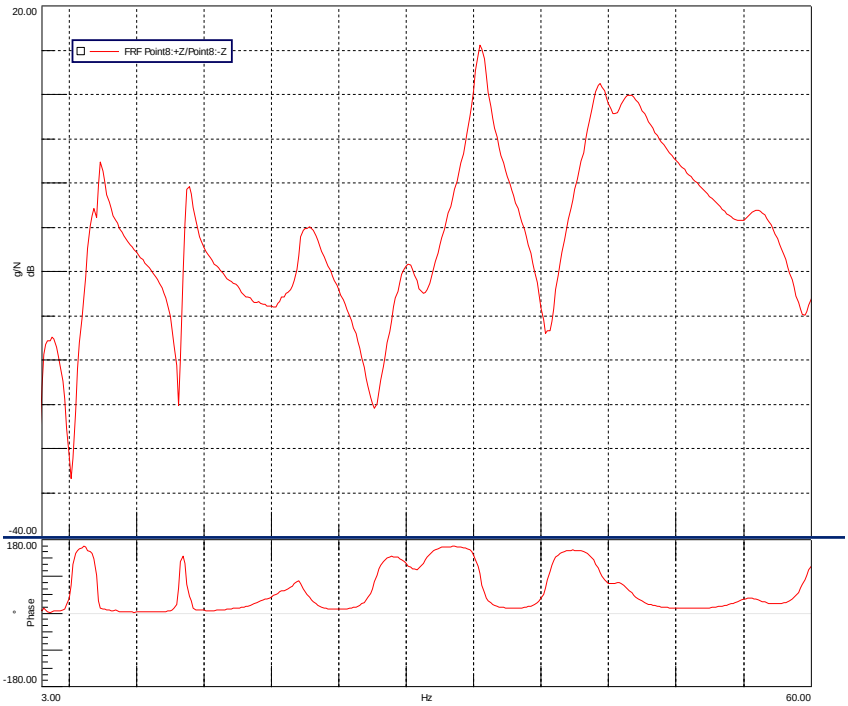

Figure 4. FRF from driving Point

4. COMBINED ACCELEROMETERS-STRAIN GAUGES GVT SETTINGS

Based on the modal identification of the wing GVT, a preliminary placement of strain and acceleration sensors was defined and is shown in Fig. 3. At all nine accelerometers are used for each semi-wing and a geometric reference accelerometer is positioned in the center of the wing on the elastic axis (provided in the stringer). The accelerometers numbered from 1-8 and 11-18 are located as close as possible to the leading edge or trailing edge of the ribs as pointed out in Fig. 5, allowing the maximization of torsion capture and to prevail overall modes. The accelerometer numbers 9

and 19 are located in the wing tips. In the horizontal stabilizer are fixed three accelerometers where two (no. 21 and 22) are in the tips and the other (no. 23) is in the middle. The accelerometer (no. 23) is attached to the top of the vertical stabilizer. In the fuselage two accelerometers (no. 24 and 25) are fixed in the two longitudinal ends. A total of 25 different positions for acceleration sensors are determined for the present configuration.

The strain gage rosettes are located near to the root of each semi-wing with the aim to capture the corresponding deformation, mainly for the first-order torsion mode. The other pair of rosettes is intended to complement the information for the first torsion modes and capture the basic features of the second order torsion modes. Four additional simple strain gauges are located as shown in order to obtain strain information for the bending modes.

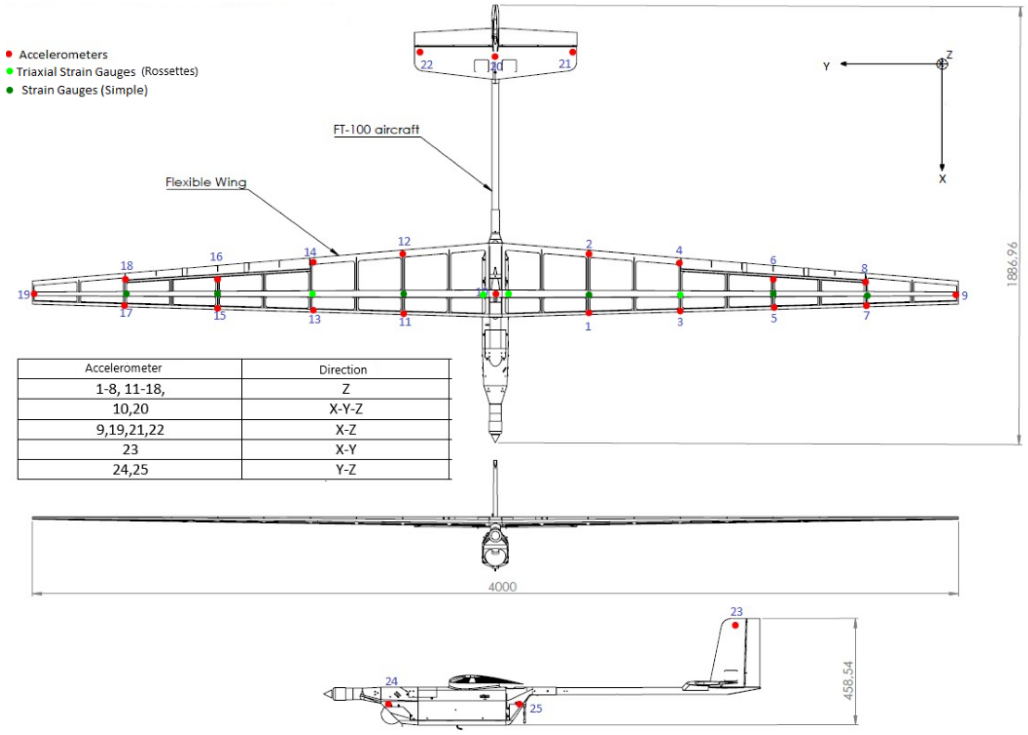

Accelerometer	Direction
1-8, 11-18,	Z
10,20	X-Y-Z
9,19,21,22	X-Z
23	X-Y
24,25	Y-Z

Figure 5. Definition and location of sensors for a combined accelerometers-strain gauges modal analysis of the flexible wing UAV.

The selected strain gauge and rosette models are CEA-06-125UW-350 CEA-06-250UR-350 respectively, both of Vishay/Micro-Measurements, they are shown in Fig. 6. The selected accelerometer model are is ADLX345. It is a low power, 3-axis MEMS accelerometer modules with both I2C and SPI interfaces. The ADLX345 features 4 sensitivity ranges from +/-2G to +/- 16G and it supports output data rates ranging from 10HZ to 3200 Hz. It is shown in Fig. 7.

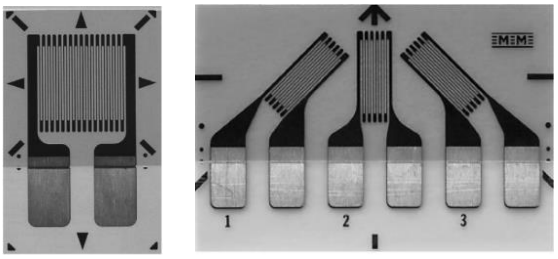

Figure 6. Strain sensors: (a) Linear strain gauge and (b) Strain gauge rossette.

Figure 7. Accelerometer

5. DATA ACQUISITION SYSTEM

In order to retrieve information of all sensors installed in the aircraft, a data acquisition system was developed. The arquitecture of such system is shown in Fig. 8.

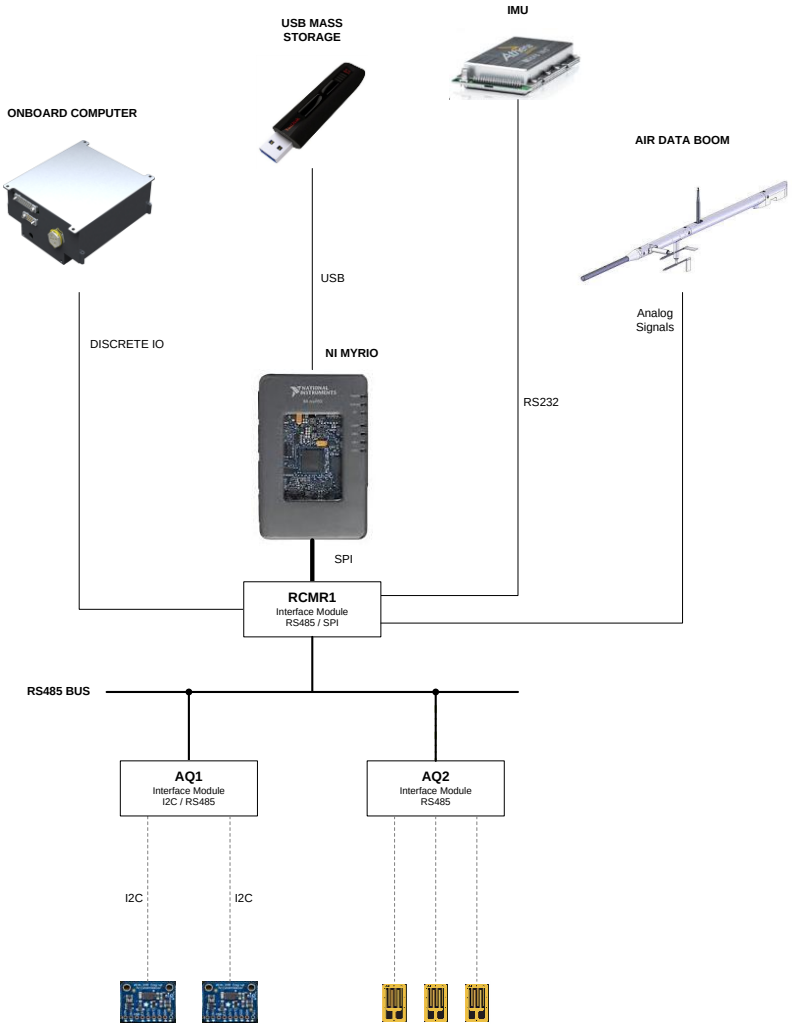

Figure 8. Data Acquisition System Arquitecture.

The heart of the data acquisition system is the National Instruments MyRio. This device concentrates the information from all the acquisition system components: accelerometers, strain gages, air-data boom, inertial navigation system and the on board computer. In order to carry the information from the acceleration and strain sensors, a RS-485 bus is provided. The National Instruments MyRio is connected to the RS-485 bus through a custom electronic hardware, or a bridge, called RCMR1, with its main function is to convert the RS-485 protocol to Serial Peripheral Interface (SPI) available in MyRio.

In the same way, as the acceleration and strain gage sensors does not have built-in RS-485 interface, custom interface hardware were developed in order to integrate the sensors to the acquisition system. The AQ1 board is the interface hardware for the Analog Devices accelerometers ADXL345. It reads the data from one or two accelerometers over I2C, each one in up to the 3 axis and sends the information to the RS-485 bus. The AQ2 board has the analog acquisition circuitry specifics for strain gages measurements. It has 18 bits analog digital converters and a Wheatstone bridge for each of the strain gages channels. The AQ2 can read up to 3 strain gages.

The inertial navigation unit communicates with National Instruments MyRio over RS-232. Further the National Instruments MyRio has analog interfaces to be connected to the air data boom in order to read the angle of attack and angle of sideslip. The latest two devices are unnecessary for this research and the related data will be used somewhere else.

The onboard computer has the ability to turn on and off the acquisition system through a discrete TTL input. All the information is stored in an USB mass storage device in TDMS format to be analyzed after the flight campaigns.

6. WING TRADITIONAL GVT RESULTS

From the initial modal tests, eight modes were identified in the frequency range from 0 to 50 Hz for the present flexible wing configuration. These modes are bending and torsional modes. The first mode is a symmetric bending mode, followed by an antisymmetric bending mode, then the second symmetric bending mode and very close in frequency a first antisymmetric torsional mode. In a future modal test campaign it will be deeply analyzed the nature, interaction or possible coupling between these two near modes. The next two identified modes correspond to the first symmetric torsional mode and the second antisymmetric bending mode. The last two identified modes are the third symmetric bending mode and a second order torsional mode. In Tab. 2 are shown the modes with their corresponding frequencies and damping. The mode shapes for a semi-wing are shown in Figs. 9 to 12.

Table 2. Identified modes from experimental modal analysis

Mode (Description)	**Freq (HZ)**	**Damping (%)**
1st Symmetric bending	7.1	4.51
1st Antisymmetric bending	13.7	1.19
2nd Symmetric bending	22.1	1.41
1st Antisymmetric Torsion	22.8	3.77
2nd Symmetric Torsion	30.3	3.04
2nd Antisymmetric bending	35.5	1.52
3rd Symmetric Bending	44.4	1.47
2nd Antisymmetric Torsion	46.4	2.42

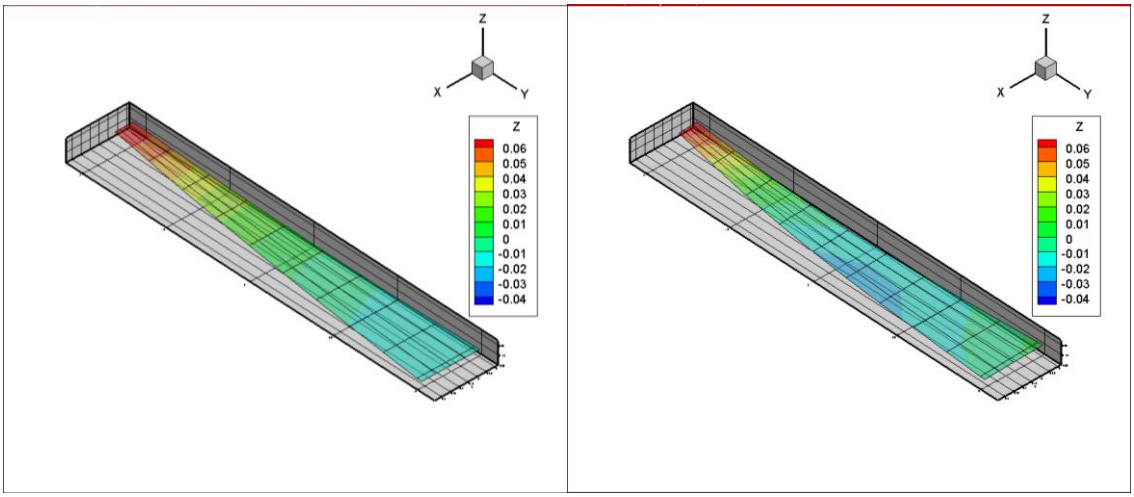

Figure 9. (a) 1st symmetric bending mode at 7.1 Hz (b) 1st antisymmetric bending mode at 13.7 Hz

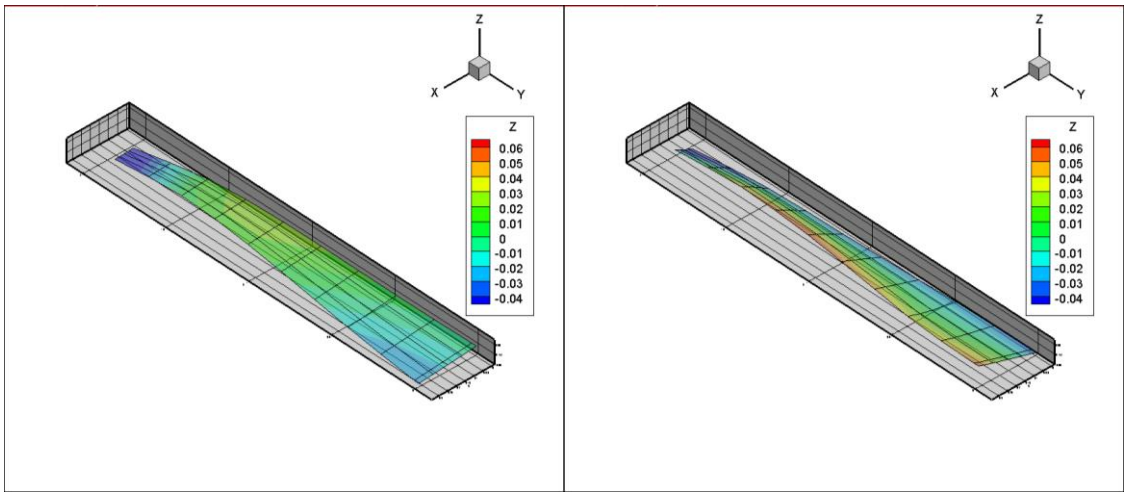

Figure 10. (a) 2nd symmetric bending mode at 22.0 Hz (b) 1st antisymmetric torsional mode at 22.8 Hz

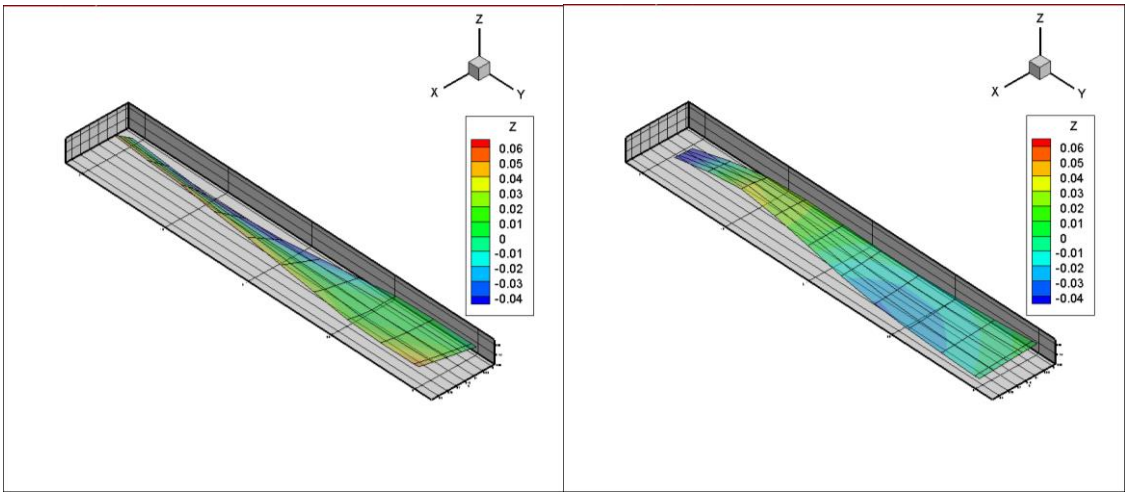

Figure 11. (a) 1st symmetric torsional mode at 30.2 Hz (b) 2nd antisymmetric bending mode at 35.5 Hz

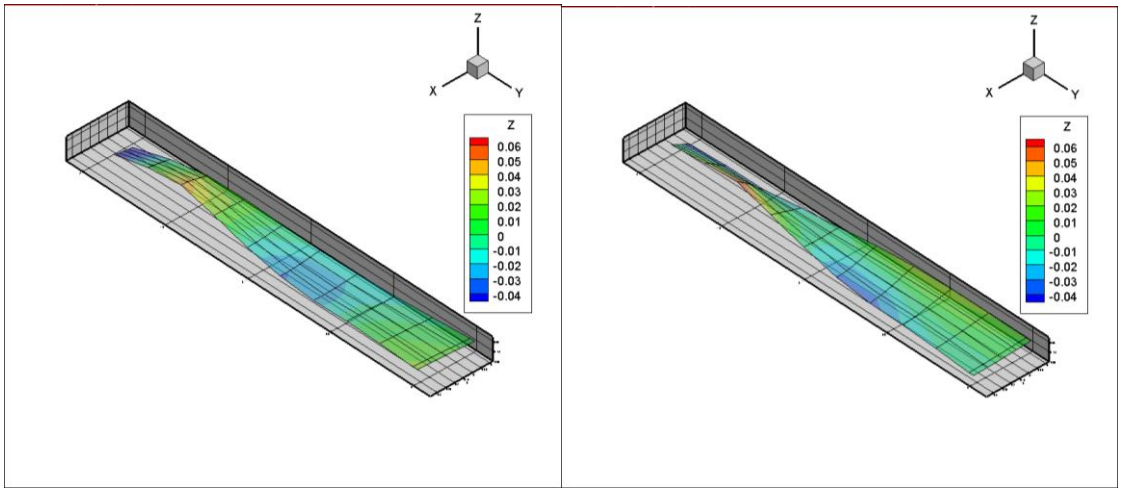

Figure 12. (a) 3rd symmetric bending mode at 44.4 Hz (b) 2nd antisymmetric torsional mode at 46.4 Hz

An AutoMAC analysis for verification of consistency of the GVT identified modes is shown in Fig. 13. It is observed that the diagonal elements are near of unity while the elements out the diagonal remaining lower than 0.4 for the worst case.

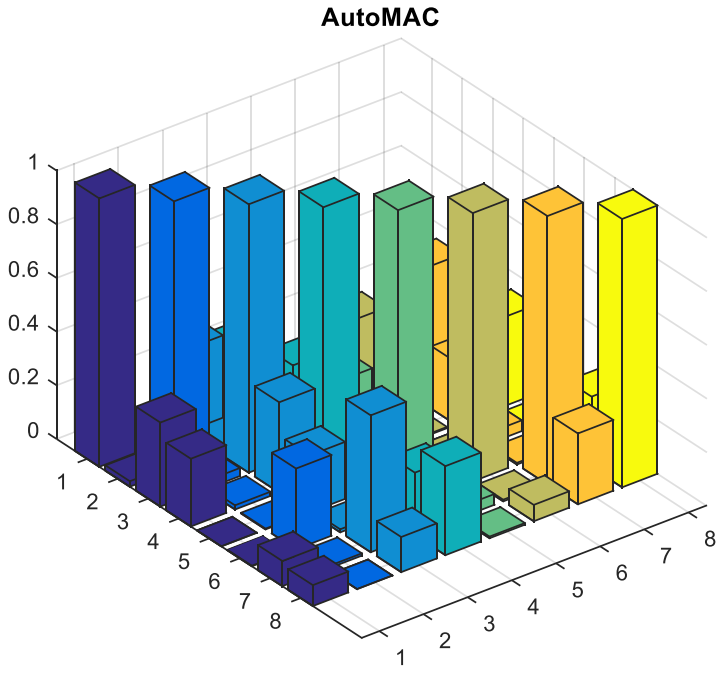

Figure 13. AutoMAC of the GVT identified modes.

7. CONCLUSION

This work presented an ongoing research to apply traditional experimental modal analysis to determine eight mode shapes and their characteristics for a flexible wing UAV. In addition, from the initial modal characterization, a test setup was planned for the application of a combined accelerometer-strain sensor GVT campaign. The modal properties obtained are very useful to perform a subsequent numerical aeroelastic analysis and to design aeroelastic inflight test experiments.

8. ACKNOWLEDGEMENTS

This work was supported in part by CAPES (Coordenação de Aperfeiçoamento de Pessoal de Nível Superior) – Brazil. The authors of this paper would like to acknowledge Professor Airton Nabarrete Ph.D., Adolfo Ph.D and all who contributed in some way for this work.

9. REFERENCES

Castillo-Zúñiga, D. F. and Góes, L. C. S., 2012 “Modal Testing of the Vector-P Unmanned Aerial Vehicle”. In *Proceedings of the 7th Brazilian Congress of Mechanical Enginnering - CONEM*. São Luiz de Maranhão, Brazil.

Castillo-Zúñiga, D. F., 2013. *Aeroelastic Analysis and Comparison with In-Flight Testing of Unmanned Aerial Vehicles*. M.Sc. thesis - Instituto Tecnológico de Aeronáutica, São Jose dos Campos, Brazil.

dos Santos, F. L. M., Peeters, B., Debille, J., Salzano, C., Goes, L. C. S. and Desmet, W., 2015. “The use of dynamic strain sensors and measurements on the ground vibration testing of an F-16 Aircraft”. In *Proceedings of the International Forum on Aeroelasticity and Structural Dynamics – IFASD2015*. Saint Petersburg, Brazil.

dos Santos, F. L. M., 2015. *Strain-Based Experimental Modal Analysis: Advances in Theory and Practice*. Ph.D, Instituto Tecnológico de Aeronáutica, São Jose dos Campos, Brazil.

Ewins, D. J., 2000. *Modal Testing: Theory, Practice and Application*. Research Studies Press Ltd, 2nd edition.

Maia, N.M.M. and Silva, J., 1997. *Theoretical and Experimental Modal Analysis.* Research Studies Press Ltd.

Manzanato. S, dos Santos, F., Peeters, B., Leblanc, B.,White, J., 2014. “Combined accelerometers-strain gauges operational modal analysis and application to wind turbine data”. In *Proceedings of the* the 9th International Conference on Structural Dynamics, *EURODYN*. P

Peeters, B., Van der Auweraer, Guillaume, P. and Leuridan, J., 2004. “The polyMAX frequency-domain method: a new standar for modal parameter estimation?”. Shock and Vibration. Vol. 11, p. 395-409.

10. RESPONSIBILITY NOTICE

The author are the only responsible for the printed material included in this paper.